Spatially Resolved 3 μm Spectroscopy of IRAS 22272+5435: Formation and Evolution of Aliphatic Hydrocarbon Dust in Proto-Planetary Nebula[1]

Miwa Goto [2,3], W. Gaessler[2,4], Yutaka Hayano[5], Masanori Iye[5], Yukiko Kamata[5], Tomio Kanzawa[2], Naoto Kobayashi[2], Yosuke Minowa[5], D. J. Saint-Jacques[6], Hideki Takami[2], Naruhisa Takato[2], Hiroshi Terada[2]

mgoto@duke.ifa.hawaii.edu

ABSTRACT

We present medium resolution 3 μm spectroscopy of a carbon-rich proto-planetary nebula IRAS 22272+5435. Spectroscopy with the Subaru Telescope adaptive optics system revealed a spatial variation of hydrocarbon molecules and dust surrounding the star. The ro-vibrational bands of acetylene (C_2H_2) and hydrogen cyanide (HCN) at 3.0 μm are evident in the central star spectra. The molecules are concentrated in the compact region near the center. The 3.3 and 3.4 μm emission of aromatic and aliphatic hydrocarbons are detected at 600–1300 AU from the central star. The separation of spatial distribution between gas and dust suggests that the small hydrocarbon molecules are indeed the source of solid material, and that the leftover gas of the grain formation are being observed near the central star. The intensity of aliphatic hydrocarbon emission relative to the aromatic hydrocarbon decreases with the distance from the central star. The spectral variation is well matched to that of a laboratory analog thermally annealed with different temperatures. It is suggested that either the thermal process after the formation of a grain, or the temporal variation of the temperature in the dust forming region is relevant to determine the chemical composition of the hydrocarbon dust around the proto-planetary nebula.

---

[1]Based on data collected at Subaru Telescope, which is operated by the National Astronomical Observatory of Japan.

[2]Subaru Telescope, 650 North A'ohoku Place, Hilo, HI 96720

[3]Visiting astronomer at the Institute for Astronomy, University of Hawaii

[4]Max-Planck-Institut für Astronomie, Königstuhl 17, Heidelberg D-69117, Germany

[5]National Astronomical Observatory of Japan, Mitaka, Tokyo 181-8588, Japan

[6]Département de physique, Université de Montréal, Montréal (Québec) H3C 3J7, Canada

Subject headings: stars: AGB and post-AGB — circumstellar matter — stars: individual (IRAS 22272+5435) — dust, extinction — ISM: evolution — infrared: ISM

1. Introduction

IRAS 22272+5435 (= HD 285858, SAO 34504) is an extremely carbon-rich protoplanetary nebula (PPN) with peculiar infrared spectral features (Kwok, Volk, & Hrivnak 1989; Geballe et al. 1992). A PPN is a transition object that left the asymptotic giant branch (AGB) for a planetary nebula (PN) though not yet hot enough to ionize the surrounding AGB ejecta. The dust in a PPN is becoming optically thin, but has not been altered in the hard UV field of PN. A carbon-rich PPN provides a best opportunity to study unprocessed solid carbon material immediately after the formation.

A classification of carbon dust in the interstellar medium (ISM) has been proposed by Geballe (1997) and Tokunaga (1997) based on the 3 μm infrared emission features (IEF). The class A sources are characterized by the intense and isolated aromatic features at 3.3 μm with occasional association of weak and sharp peaks in the 3.4–3.5 μm region. They are the most common IEF sources vastly observed toward young stellar objects (YSO), H II regions, PN, reflection nebulae, diffuse interstellar medium and extragalactic sources (Tokunaga et al. 1991; Sloan et al. 1997; Jourdain de Muizon, D'Hendecourt, & Geballe 1990; Sellgren 1983; Tanaka et al. 1996; Moorwood et al. 1996). The class B sources are characterized by a broad and prominent aliphatic features at 3.4 μm accompanied with the 3.3 μm aromatic features. The class B IEF has been exclusively found toward PPN with extremely carbon-rich chemistry typified by IRAS 22272+5435 (Geballe & Van der Veen 1990; Geballe et al. 1992). Simultaneous presence of aromatic and aliphatic features in class B sources makes a good laboratory for the study of transition of the chemical composition of hydrocarbons.

Another advantage to observe a PPN is that the history of the dust formation is locked in a spatial distribution of the material. Since PPN are less developed than PN, most of them are spatially unresolved. However, the dust distribution around IRAS 22272+5435 has been well studied by the subarcsecond mid-infrared imaging (Meixner et al. 1997; Dayal et al. 1998; Ueta et al. 2001), optical imaging with *Hubble Space Telescope*/Wide Field Planetary Camera 2 (*HST*/WFPC2) (Ueta, Meixner, & Bobrowsky 2000), and near-infrared polarimetric imaging (Gledhill et al. 2001). Ueta, Meixner, & Bobrowsky (2000) classified IRAS 22272+5435 into a group of PPN that are optically thin. It then ensures an unobscured vision into the central part of the nebula.

Although observing at 3 μm is essential to assess the chemical composition of the carbon dust, a drawback is that the emitting region is physically more compact than at longer wavelengths. In addition the contribution of the direct and scattered light from the central star is not negligible in the 3 μm region. Not only to resolve the dust emission region, but also for the high dynamic range required to discriminate faint dust emission from the central star, spectroscopy using adaptive optics system (AO) is integral for the observation. The goal of this paper is to better understand how the hydrocarbon dust forms around a carbon-rich evolved star, and how they are processed before dissipating into the local ISM based on the high spatial resolution spectroscopy afforded by AO.

2. Observation

The spectroscopic observation was made on UT 2001 July 13 using the Infrared Camera and Spectrograph (IRCS; Tokunaga et al. 1998; Kobayashi et al. 2000) at the 8.2 m Subaru Telescope in conjunction with the AO system (Takami et al. 1998; Gaessler et al. 2002). The Subaru AO is a 36-element curvature system installed at the front end of the telescope Cassegrain port. A medium resolution grism was used with a $0\farcs30$ slit in the 58 mas camera section to provide spectra from 2.84 to 4.18 μm with resolving power of 600–800. The visible central star was used as the wavefront reference source for the AO system. The position angle of the slit was 56° along the elongation in the mid-infrared image that corresponds to an equatorial density enhancement of the nebula (Ueta et al. 2001). The spectra were recorded by nodding the tip-tilt mirror inside the AO system by 2″ along the slit to subtract the sky emission and dark current images. The total on-source integration time was 720 s. A nearby F8V star HR 8472 was observed as a spectroscopic standard at similar airmass. The spectroscopic flat field was obtained at the end of the night with a halogen lamp.

3. Data Reduction and Result

We obtained the one dimensional spectra of IRAS 22272+5435 using the IRAF[7] aperture extraction package. The aperture width was about equal to the FWHM of the spatial profile (4-pixel or $0\farcs23$). We set the extraction apertures at the central star and another 14 locations along the slit (Figure 1). We found the spectra recorded at the nodding position A and B

[7]IRAF is distributed by the National Optical Astronomy Observatories, which are operated by the Association of Universities for Research in Astronomy, Inc., under cooperative agreement with the National Science Foundation.

to be slightly different. The most likely reason for this is that the mirror nodding axis was not precisely straight to the slit, and we observed slightly different part of the nebula. The data obtained at position A and B were reduced separately. The wavelength calibration was performed by fitting over 60 telluric absorption lines in the 3 μm region. The flux calibration relative to the standard star was made assuming the intrinsic spectrum of a F8V star is represented by a Planck function of $T_{\rm eff} = 6100$ K (Tokunaga 2000). The hydrogen recombination lines in the standard star spectrum were fit with a Gaussian function and subtracted before dividing. The detail of the reduction can be found elsewhere (Goto et al. 2002).

The result is shown in Figure 2 after normalized to the continuum at 3.5 μm. No hydrocarbon emission feature is seen at the position of the central star. Instead we observe absorption bands with the hydrocarbon emission bands becoming evident only at $0\farcs35$ from the central star. The integrated intensity of the hydrocarbon emission bands is consistent with that of $5''$ aperture spectroscopy formerly reported by Geballe et al. (1992). The absence of hydrogen recombination lines at 3.74 μm (Pfγ) and 4.05 μm (Brα) ensures that no H II region has developed at the center of the nebula. The spectrum continuum is approximately represented by a power law. The continuum flux around the central star is most likely the scattered light by large dust grains in the nebula superposed on the halo component of the point spread function of the central star. The continuum subtracted spectra are shown in Figure 3.

4. Discussion

4.1. Molecular Absorption Features Near The Center

A wealth of absorption features are found in the spectra of IRAS 22272+5435 close to the central star. The carbon atoms consisting C-H bonds have one of *sp*, sp^2 or sp^3 hybridized orbitals, in which triple, double and single bonds connect the carbon with adjacent atoms. The stretching vibration mode of different C-H bonds shows up as various band structures in the 3 μm region. The individual ro-vibrational transition lines are not resolved with the present spectral resolution, and the higher resolution spectroscopy should be in order for the solid identification of the absorption lines. The only exception is the absorption bands at 3.0 μm identified with the combination of P and R branches of *sp* C-H bonds in C_2H_2 and HCN. Figure 4 shows the same molecular features in CRL 618 (Chiar et al. 1998) and those computed with HITRAN database (Rothman et al. 1998).

The molecular absorption features are evident close to the central star, but they are

abruptly disappear at 0.″47 or 750 AU (d = 1.6 kpc is assumed based on the private communication with Nakashima 2002). The broad emission bands at 3.3 and 3.4 μm become strong in turn at 600 AU (Figure 3). This is the first time that both of the hydrocarbon gas and dust are observed in a circumstellar environment in clearly separated locations. It indicates the hydrocarbon molecules are indeed the source of the solid dust material, and that the molecular gas failed to be involved with the grain formation is being observed near the central star.

4.2. Hydrocarbon Dust Emission at 3.3–3.4 μm

The most common IEF in the ISM is class A type emission ubiquitously observed where the carbon dusts are exposed to hard UV field. The emission carrier has been attributed to the aromatic species (Duley & Williams 1981) such as neutral and ionized polycyclic aromatic hydrocarbons (PAH; Léget and Puget 1984; Allamandola, Tielens, & Barker 1985; Allamandola, Tielens, & Barker 1989 and reference therein). The 3.3 μm feature matches with the ro-vibrational band of the stretching vibration of aromatic sp^2 C-H bonds. While the class A IEF is observed with hot excitation sources with $T_{\rm eff} > 20000$ K, the central stars of class B sources are typically F–G type supergiants whose effective temperature is $T_{\rm eff} = 4500$–7000 K. The radiation environment of class B sources is much benign with less UV photons available. The aromatic molecules absorbs UV-visible photons with a long wavelength cut-off. The larger molecules in size has longer cut-off wavelength (Desért, Boulanger, & Puget 1990; Schutte, Tielens, & Allamandola 1993). The soft radiation field yet strong emission of class B sources implies larger hydrocarbons are responsible than those of class A sources.

What distinguish class B spectra most clearly from class A IEF is a broad and intense emission at 3.4 μm. It was once proposed that a hot band of anharmonic oscillation of aromatic C-H bonds is responsible (Barker, Allamandola, & Tielens 1987). However, the weakness or absence of overtone band at the 1.6–1.8 μm region makes this hypothesis less likely (Magazzu, & Strazzulla 1992; Siebenmorgen & Peletier 1993; Geballe et al. 1994). Instead Schutte, Tielens, & Allamandola (1993) proposed that the aliphatic C-H bonds of superhydrogenated benzene rings account for the 3.4 μm emission. Hydrogenated PAH (H_n-PAH) is rich in sp^3 C-H bonds that the double bonds in the benzene rings are partially saturated by extra attachment of hydrogens to the peripheral carbons. Bernstein, Sandford, & Allamandola (1996) has shown that some H_n-PAH have similar absorption peaks that agree well with 3.4–3.5μm features of a class A source Orion bar. Joblin et al. (1996) argues that the aliphatic C-H bonds, in particular -CH_2 in long chains or cyclic aliphatic hydrocarbons, best match with the strong 3.42 μm features of class B source IRAS 05341+0852.

In the mid-infrared region IRAS 22272+5435 shows two broad emission features near 8 μm and 12 μm (Buss et al. 1993), which is in contrast with typical class A IEF (Sloan et al. 1999). Allamandola, Hudgins, & Sandford (1999) tried several laboratory compounds of PAH to reproduce IEF of class A and class B sources. They suggested that there is a systematic difference in the character of aromatic species required to fit the IEF in the two different environments. The class A IEF is mostly reproducible by compounds of cations of stable PAH species, while neutral and less stable PAH species should have larger contribution to better match the broad features of class B sources.

Specific chemical materials have been proposed for the class B IEF carriers by many authors. Those substances are more in solid form, and the laboratory spectroscopy indicates they are rich in sp^3 hybridized bonds. These are more common characteristic with amorphous carbons, totally fit in the above tweaks required for the conventional aromatic species, namely, larger, more neutral, and more aliphatic materials for class B IEF. The possible carriers presented so far are all successful in reproducing the spectral shape from 3.3 to 3.4 μm. These include a mixture of PAH molecules fully re-processed by energetic hydrogen plasma (Beegle, Wdowiak, & Arnoult 1997; Arnoult, Wdowiak, & Beegle 2000), carbon nanoparticles produced by laser pyrolysis of C_2H_4 and C_4H_6 (Herlin et al. 1998) or C_2H_2 (Schnaiter et al. 1999), hydrogenated amorphous carbon prepared by eximer laser ablation of graphite in a hydrogen rich atmosphere (Scott, Duley, & Jahani 1997; Grishko & Duley 2000), and quenched carbonaceous composite produced by plasma deposition technique with CH_4 (Sakata et al. 1990; Goto et al. 2000). Semianthracite coal grain (Guillois et al. 1996) is also successful in reproducing the aliphatic band at 3.4 μm and substructures in the mid-infrared feature and overall continuum shape. Since there is no unique laboratory analog, we refer the carrier of the class B emission features at 3.3–3.4 μm as " hydrocarbon dust" in the following text. The hydrocarbon dust is rich in both aromatic and aliphatic C-H bonds.

4.3. Variation of Aliphatic and Aromatic Abundance

Figure 5 shows the emission feature at 600 to 1300 AU from the central star at the northeast of the nebula. The relative intensity of the aliphatic feature at 3.4 μm to aromatic feature at 3.3 μm decreases with the distance from the central star. We discuss two processes that could modify the relative abundance of the aliphatics to the aromatics.

First we examine the formation of the aliphatic C-H bonds on the surface of carbon particles. Mennella et al. (1999) demonstrated that sp^3 hybridized C-H bonds are newly formed by exposing pure carbon particles to atomic hydrogen atmosphere. The activated

aliphatic band successfully reproduces the 3.4 μm absorption feature observed toward the Galactic center. They discuss that the carrier responsible for the 3.4 μm absorption ubiquitously observed toward highly reddened objects does not originate in cold dark clouds as has been proposed by Greenberg et al. (1995), but in the diffuse ISM where the destruction of C-H bonds by UV photolysis is equilibrated by rehydrogenation with ample atomic hydrogen (Mennella et al. 2001, 2002). Tielens et al. (1994) proposed a similar mechanism for the formation of aliphatic C-H bonds by hydrogenation of graphite surface amorphitized by the ion bombardment in the interstellar shocks. The process supposedly plays an important role in the production of the 3.4 μm absorption feature in the Galactic center sources (Schnaiter et al. 1999). Chiar et al. (1998) proposed that the shocks caused by the fast wind at the last stage of the post-AGB evolution is relevant to form the 3.4 μm absorption carriers in CRL 618.

However, the freshly formed aliphatic bands do not match the *emission* feature we observed. In Figure 6 we compare the emission feature of IRAS 22272+5435 with the absorption features of carbon particles from Mennella et al. (1999), CRL 618 (Chiar et al. 1998) and Galactic center (Chiar et al. 2000) as well as the laboratory analog of Goto et al. (2000). Indeed the hydrogenated nano-sized carbon particles of Mennella et al. (1999) well reproduce the observed *absorption* band, the discrepancy with IRAS 22272+5435 is obvious, indicating different carriers. Considering CRL 618 is a PPN more evolved than IRAS 22272+5435 with a compact H II region and a hot B0 star at the center of the nebula, the availability of UV might be critical to produce the particular chemical composition of the absorbing aliphatic hydrocarbons.

The thermal annealing of aliphatic material better fits the observed spectral variation. Figure 5 shows the 3 μm spectra of a laboratory analog of hydrocarbon dust subjected to thermal annealing at different temperatures (Goto et al. 2000). The model carbon dust produced by plasma vapor deposition method of CH_4 has rich sp^3 hybridized C-H bonds when it is deposited. As the annealing temperature becomes hotter in the post processing, the substance is dehydrogenated and graphitized. It gradually acquires strong continuum absorption, less prominent spectral features, and weak aliphatic features relative to the aromatic one. The thermal transformation of the aliphatic material is well studied in laboratory experiments with amorphous carbon films (Robertson 1991; Bounouh et al. 1995). Similar spectral alterations have been also reported with hydrogenated amorphous carbons (Scott & Duley 1996; Scott, Duley, & Jahani 1997; Grishko & Duley 2000; Mennella et al. 1996). The resemblance between the laboratory and the observed spectra indicates similar process takes place in IRAS 22272+5435.

4.4. Thermal Process

4.4.1. Heat source

For the thermal annealing of aliphatic material to take place, we need an adequate heat source with raw material. The chemical composition of the thermally processed material is sensitive to the annealing temperature. The aliphatic to aromatic ratio observed in IRAS 22272+5435 indicates that the hydrocarbon dust has undergone the heating about 760 K (Figure 5).

On the investigation of heating mechanisms, we first assume the thermal annealing is currently in progress at $\sim$ 1000 AU away from the star where the hydrocarbon emission is being observed. The equillibrium temperature at 1000 AU is too cool for annealing to happen. Ueta et al. (2001) presented $T_{\rm dust}$ = 200 K at 800 AU from the star solving two dimensional radiation transfer model, which is again too cool for the thermal annealing. The shock heating could be an alternative heat source, however, no sign of shock-induced molecular hydrogen emission has been observed in the 2 μm spectrum (Hrivnak, Kwok, & Geballe 1994).

The heating mechanism is not necessarily a thermal equilibrium process. The thermal fluctuation or stochastic heating occurs when the energy of single incident photon exceeds the total heat capacity of a grain. As no hydrogen recombination lines are detected in IRAS 22272+5435, no photons are available more energetic than Lyα or $h\nu$ = 10.2 eV. It is found that a grain should be smaller than 6 Å in radius ($N_C < 100$) to be heated to 760 K by a single Lyα photon. We use the empirical specific heat of graphite measured at low temperature (Touloukian & Buyco 1970) and the graphite mass density 2200 kg m^{-3} for the estimation of the heat capacity. This is very small as a solid particle, however, grains of this size have been considered as a common constituent of reflection nebulae to account for the hot blackbody continuum of about 1000 K (Sellgren 1984).

Alternatively, as a PPN is a mass losing object, the observed spatial variation could be interpreted as a record of history of grain production of the central star. The changing chemical composition at the outer circumstellar shell could represent the temporal transition of hydrocarbon output during the evolution of PPN. The possible mode-switching in the production of dust has been proposed by Buss et al. (1993); Geballe (1997); Kwok, Volk, & Hrivnak (1999); Kwok, Volk, & Bernath (2001) to account for the systematic difference of the IEF in PN and their progenitor PPN. Thus, the thermal processing is not necessarily a current ongoing event. Actually the most obvious heat source in the nebula is the central star and the warm circumstellar shell close to it. The particular chemical composition, or a sign of thermal processing, would be acquired when a grain was still in the warm environment

near the star. We will call the inhomogenious chemical composition as a consequence of temporal transition of grain formation "old record" scenario. In the scenario the thermal processing was completed close to the central star, and is being observed at present when the dust grains with varying chemical compositions are blown off to the 1000 AU away from the star.

We will consider the two heating scenarios in the following discussion, (1) the ongoing stochastic heating of a very small grain, and (2) the old record scenario that the spatial variation of the chemical compositions originates in the past at the grain formation in the warm region at the vicinity of the central star.

4.4.2. Preserving aliphatic material

The immediate problem with the stochastic heating scenario is how the aliphatic material could survive through the warmer environment closer to the central star. The physical conditions are more preferable for active thermal annealing there, for instance at the temperature of carbon condensation the aliphatic material should be totally graphitized.

Before discussing the preservation of the aliphatic material, first we consider the location where the ultra small grains could form. Because of the lack of efficient destructive mechanism, a grain monotonically grows in the mass loss wind as it travels through the circumstellar shell (Gail & Sedlmayr 1988). Thus, a small grain can be only formed at the outer region of the envelope where the grain growth is very inefficient otherwise the final dimension would be too large (Figure 7). Dominik, Gail, & Sedlmayr (1989) found that while most of the grains are nucleated at 1–2 R_* from the star and keep growing until it becomes as large as 0.01–0.1 μm, the population of small grains of carbon content $N_C = 100$ should not be nucleated at 7 R_* or closer to the central star. The temperature there falls down well below 600 K (Gail & Sedlmayr 1987). It is cool enough to allow the aliphatic C-H bonds to be preserved.

In the old record scenario we do not have to assume the ultra small grains. Most of the grains are formed in a thin shell near the sonic point 1–2 R_* from the star. The nucleation and growth rates are very high there. However, grain formation is not an instantaneous event. Although the growth rate drops by orders of magnitude, a grain keeps growing even at tens of stellar radii from the star until the source gas is completely depleted or diluted (Dominik, Gail, & Sedlmayr 1989). This means that the outermost layer of a grain particle is formed in the cool region where thermal processing no longer occurs. Thus, while the inner core formed in the warmer region is already graphitized, the fresh surface of a grain is most

likely covered by the aliphatic C-H bonds (Figure 7). The growth of "amorphous carbon mantle" in the cool (< 1100 K) mass loss wind has been discussed by Gail & Sedlmayr (1984).

4.4.3. Mass loss history

We have heat sources and the raw material ready to apply the thermal treatment. In observation we have less processed material inside, and more processed outside. We discuss how the observed spatial variation of hydrocarbon features could be possiblly produced.

We start with a gradual annealing of a small grain when it travels outward in the circumstellar shell. The incidence of the Lyα photon per grain from G5Ia central star at the distance of 1000 AU can be predicted using the stellar spectral model of Kurucz (1979). Assuming all photons of $\lambda \leq 1215$Å are converted to Lyα and the total luminosity of the central star to be $1.3\times10^4 L_\odot$ (Ueta et al. 2001), the photon rate to a 6 Å particle turns out about once in thousands years. However, it critically depends on the wavelength range we take. For instance if we count the photons $\lambda \leq 1500$ Å, the incidence rate jumps up to once in every 5 years. It drops by an order or two when visible extinction of $A_V = 1$ is applied. At each incidence a grain cools down in approximately 10^{-1} s emitting as a blackbody. As a grain is blown off roughly 1 AU per year if 10 km s^{-1} mass loss velocity is assumed, the region of our interest 600–1300 AU from the star corresponds to ∼700 yrs for a grain to go across. The Lyα photon rate ($\lambda \leq 1215$Å) without extinction does not contradict with the grain traveling time. The higher fraction of the dust particles have experienced energetic photon incidence in the outer region than in the inner region because they have been soaked in the radiation field longer. Hence, we would see more thermally annealed grains closer to the edge of the nebula. However, we have to be cautious about the coincidence of the time scale. First we implicitly assumed the effective temperature of the central star does not significantly change during the relevant period of the time, which is not a trivial issue. Second the re-organization of the carbon frameworks may not finish in an instant, but may take a finite period of time until the aliphatic to aromatic transformation is settled down. When the alteration time scale is longer than the cooling time, a single Lyα photon is insufficient to transform the chemical composition of the entire grain. Further discussion on the gradual annealing scenario would be premature until the microscopic processes of thermal annealing as well as the effect of the central star evolution is fully understood.

A size variation with distance from the star may provide a solution to account for the spatial variation of chemical composition. Suppose that there are dominant population of small grains further away from the star, they are more processed than inner ones because

a smaller grain reaches higher temperatures when heated with same energy input. Such a size variation with the distance from the star have been often observed in other PPN (e.g., Sahai et al. 1998). As the higher mass loss rate results in the larger grain size (Krüger & Sedlmayr 1997), the accelerating mass loss at the end of AGB might be relevant to produce the hypothetical grain size distribution.

On the other hand in the old record scenario the assumed grain size is large enough to keep grains from thermal fluctuation. Thus, once the grain growth ceased near the star ($\sim$ 20 R_*), the chemical composition of the grain surface is locked unchanged during the traverse in the mass loss wind. Then the variation of the spectral feature we observed at 1000 AU from the star simply reflects how the grain surface were composed near the star. If the time scale of the grain growth is slow, it may keep growing at the cool region in the outer circumstellar shell, gradually building more aliphatic-rich mantles on the surface. In contrast if the source gas quickly depletes closer to the star, a grain stops growing earlier in the warm region and the surface composition remains mainly graphitic. The observed spatial variation implies a history of the gradual switching of these dust formation modes. However, dust formation models available at present are based on the stationary mass loss wind, which is ineffective to predict the temporal variation of chemical composition in dust production. The mass loss rate is very sensitive to the stellar parameter at the end of the AGB phase (e.g., Willson 2000). In particular in the superwind phase the mass loss shows complicated temporal variation strongly dependent on the initial mass of stars (Wachter et al. 2002; Schröder, Winters, & Sedlmayr 1999). In order to fully understand how the time variable mass loss affects on the chemical properties of dust, how those dust grains build up a heterogeneous spatial structure around the central star, and eventually how the spectrum of chemical composition of dust is going to be which carbon-rich, late-type stars return to the ISM, further theoretical and observational studies are much awaited.

5. Summary

We presented spatially resolved 3 μm spectroscopy of the proto-planetary nebula I-RAS 22272+5435 that reveals the different distribution of the hydrocarbon gas and dust. The main conclusions are follows,

1. The acetylene (C_2H_2) and hydrogen cyanide (HCN) absorption is found in the central star spectrum at 3.0 μm. The molecules are highly concentrated in the compact region at the center.

2. The 3.3 and 3.4 μm hydrocarbon dust emission is detected at 600–1300 AU from the

star. The spatial separation of C_2H_2 and hydrocarbon dust is observed for the first time, and it reinforces the classical view of the dust formation.

3. We found the relative intensity of aliphatic feature at 3.4 μm to aromatic feature at 3.3 μm decreases with the distance from the star. The spatial variation of the spectral feature is well reproduced by the spectra of a laboratory analog of carbon dust. The thermal process is likely to account for the spectral variation.

4. We suggested the stochastic heating of very small grains ($a < 6$ Å) or the grain surface composition at the end of grain growth would explain the changing aliphatic and aromatic spectral features. In both cases the time dependent mass loss profile should be the key to reproduce the spatial variation.

We thank all the staff and crew of the Subaru Telescope and NAOJ for their valuable assistance obtaining these data and continuous support for IRCS and Subaru AO construction. Takashi Kozasa and Masao Saito are appreciated for their useful suggestions in the discussion. We are grateful to V. Mennella and collaborators for making their data available for use in Figure 6. We are also grateful to J. E. Chiar and collaborators for kindly allow us to reproduce their data in Figure 4 and Figure 6. Special thanks goes to A. T. Tokunaga for many inspiring discussions and enduring encouragement during the writing. We thank the anonymous referee for the helpful comments that makes the manuscript more consistent and readable. M. Goto is supported by a Japan Society for the Promotion of Science fellowship. Last, but not least, we wish to express our appreciation for those of Hawaiian ancestry on whose sacred mountain we are privileged to be guests.

REFERENCES

Allamandola, L., J., Tielens, A. G. G. M., & Barker 1985, ApJ, 290, L25

Allamandola, L., J., Tielens, A. G. G. M., & Barker 1989, ApJS, 71, 733

Allamandola, L. J., Hudgins, D. M., & Sandford, S. A. 1999, ApJ, 511, L115

Arnoult, K. M., Wdowiak, T. J., & Beegle, L. W. 2000, ApJ, 535, 815

Barker, J. R., Allamandola, L. J., & Tielens, A. G. G. M. 1987, ApJ, 315, L61

Beegle, L. W., Wdowiak, T. J., & Arnoult, K. M. 1997, ApJ, 486, L153

Bernstein, M. P., Sandford, S. A., Allamandola, L. J. 1996, ApJ, 472, L127

Bounouh, Y., Théye, M. L., Dehbi-Alaoui, A., Matthews, A., & Stoquert, J. P. 1995, Phys. Rev. B, 51, 9597

Buss, R. H., Jr., Tielens, A. G. G. M., Cohen, M., Werner, M. W., Bregman, J. D., & Witteborn, F. C. 1993, ApJ, 415, 250

Chiar, J. E., Pendleton, Y. J., Geballe, T. R., & Tielens, A. G. G. M. 1998, ApJ, 507, 281

Chiar, J. E., Tielens, A. G. G. M., Whittet, D. C. B., Schutte, W. A., Boogert, A. C. A., Lutz, D., Van Dishoeck, E. F., & Bernstein , M. P. 2000, ApJ, 537, 749

Dayal, A., Hoffmann, W. F., Bieging, J. H., Hora, J. L., Deutsch, L. K., & Fazio, G. G. 1998, ApJ, 492, 603

Desért, F.-X., Boulanger, F. & Puget, J. L. 1990, A&A, 237, 215

Duley, W. W., & Williams, D. A. 1981, MNRAS, 196, 269

Dischler, B., Bubenzer, A., & Koidl, P. 1983, Solid State Comm., 48, No. 2, 105

Dominik, C., Gail, H.-P., & Sedlmayr, E. 1989, A&A, 223, 227

Gaessler, W. et al. 2002, Proc. SPIE, 4494, 30

Gail, H.-P. & Sedlmayr, E. 1984, A&A, 132, 163

Gail, H.-P. & Sedlmayr, E. 1987, A&A, 171, 197

Gail, H.-P. & Sedlmayr, E. 1988, A&A, 206, 153

Geballe, T. R. & Van der Veen, W. E. C. J. 1990, A&A, 235, L9

Geballe, T. R., Tielens, A. G. G. M., Kwok, S., & Hrivnak, B. J. 1992, ApJ, 398, L89

Geballe, T. R., Joblin, C., D'Hendecourt, L. B., Jourdain de Muizon, M., Tielens, A. G. G. M., & Leger, A., ApJ, 434, L15

Geballe, T. R. 1997, in *From Stardust to Planetesimals*, ASP Conf. Ser., 122, ed. Y. J. Pendleton & A. G. G. M. Tielens (San Francisco: ASP), 119

Gledhill, T. M., Chrysostomou, A., Hough, J. H., & Yates, J.A. 2001, MNRAS, 322, 321

Goto, M., Maihara, T., Terada, H., Kaito, C., Kimura, S., & Wada, S. 2000, A&AS, 141, 149.

Goto, M., Kobayashi, N., Terada, H., & Tokunaga, A. T. 2002, ApJ, 572, 276

Greenberg, J. M., Li, A., Mendoza-Gómez, C. X., Schutte, W., A., Gerakines, P. A., & De Groot, M. 1995, ApJ, 455, L177

Grishko, V. I. & Duley, W. W. 2000, ApJ, 543, L85

Guillois, O., Nenner, I., Papoular, R., & Reynaud, C. 1996, ApJ, 464, 810

Herlin, N., Bohn, I., Reynaud, C., Cauchetier, M., Galvez, A., & Rouzaud, J.-N. 1998, A&A, 330, 1127

Hrivnak, B.J., Kwok, S., & Geballe, T. R. 1994, ApJ, 420, 783

Joblin, C., Tielens, A. G. G. M., Allamandola, L. J., & Geballe, T. R. 1996, ApJ, 458, 610

Jourdain de Muizon, M., D'Hendecourt, L. B., & Geballe, T. R. 1990, A&A, 227, 526

Kobayashi, N. et al. 2000, Proc. SPIE, 4008, 1056

Kurucz, R. L. 1979, ApJS, 40, 1

Krüger, D., & Sedlmayr, E. 1997, A&A, 321, 557

Kwok, S., Volk, K. M., & Hrivnak, B. J. 1989, ApJ, 345, 51

Kwok, S., Volk, K., & Hrivnak, B. J. 1999, A&A, 350, L35

Kwok, S., Volk, K., & Bernath, P. 2001, ApJ, 554, L87

Léger, A., & Puget, J. L. 1984, A&A137, L5

Magazzu, A., & Strazzulla, G. 1992, A&A, 263, 281

Meixner, M., Skinner, C. J., Graham, J. R., Keto, E., Jernigan, J. G., & Arens, J. F. 1997, ApJ, 482, 897

Mennella, V., Colangeli, L., Palumbo, P., Rotundi, A., Schutte, W., & Bussoletti, E. 1996, in *From Stardust to Planetesimals: Contributed Papers*, NASA Conference Publication 3343, eds. M. E. Kress, A. G. G. M. Tielens & Y. J. Pendleton, 109

Mennella, V., Brucato, J. R., Colangeli, L., & Palumbo, P. 1999, ApJ, 524, L71

Mennella, V., Muñoz Caro, G. M., Ruiterkamp, R., Schutte, W. A., Greenberg, J. M., Brucato, J. R., & Colangeli, L. 2001, A&A, 367, 355

Mennella, V., Brucato, J. R., Colangeli, L., & Palumbo, P. 2002, ApJ, 569, 531

Moorwood, A. F. M., Lutz, D., Oliva, E., Marconi, A., Netzer, H., Genzel, R., Sturm, E., & de Graauw, T. 1996, A&A, 315, L109

Robertson, J. 1991, Prog. Solid St. Chem. 21, 199

Rothman, L. S., et al. 1998 Journal of Quantitative Spectroscopy and Radiative Transfer, 60, 665

Sahai, R., Hines, D. C., Kastner, J. H., Weintraub, D. A., Trauger, J. T., Rieke, M. J., Thompson, R. I., & Schneider, G. 1998, ApJ, 429, L163

Sakata, A., Wada, S., Onaka, T., & Tokunaga, A. T. 1990, 353, 543

Schnaiter, M., Henning, Th., Mutschke, H., Kohn, B., Ehbrecht, M., & Huisken, F. 1999, ApJ, 519, 687

Scott, A. D., & Duley, W. W. 1996, ApJ, 472, L123

Scott, A. D., Duley, W. W., & Jahani, H. R. 1997, ApJ, 490, L175

Schröder, K.-P., Winters, J. M., & Sedlmayr, E. 1999, A&A, 349, 898

Schutte, W. A., Tielens, A. G. G. M., & Allamandola, L. J. 1993, ApJ, 415, 397

Sellgren, K., Werner, M. W., & Dinerstein, H. L. 1983, ApJ, 271, L13

Sellgren, K. 1984, ApJ, 277, 623

Siebenmorgen, R., & Peletier, R. F. 1993, A&A, 279, L45

Sloan, G. C., Bregman, J. D., Geballe, T. R., Allamandola, L. J., & Woodward, C. E. 1997, ApJ, 474, 735

Sloan, G. C., Hayward, T. L., Allamandola, L. J., Bregman, J. D., Devito, B., Hudgins, D. M. 1999, ApJ, 513, L65

Takami, H., Takato, N., Otsubo, M., Kanzawa, T., Kamata, Y., Nakashima, K., & Iye, M. 1998, Proc. SPIE, 3353, 500

Tanaka, M., Matsumoto, T., Murakami, H., Kawada, M., Noda, M., & Matsuura, S., 1996, PASJ, 48, L53

Tielens, A. G. G. M., McKee, C. F., Seab, C. G., & Hollenbach, D. J. 1994, ApJ, 431, 321

Tokunaga, A. T., Sellgren, K., Smith, R. G., Nagata, T., Sakata, A., Nakada, Y. 1991, ApJ, 380, 452

Tokunaga, A. T. 1997, in *Diffuse Infrared Radiation and the IRTS*, ASP Conf. Ser., 124, ed. H. Okuda, T. Matsumoto, & T. Roellig (San Francisco: ASP), 149

Tokunaga, A. T. et al. 1998, Proc. SPIE, 3354, 512

Tokunaga, A. T. 2000, in *Allen's Astrophysical Quantities*, ed. A. N. Cox, (4th ed., New York: Springer)

Touloukian, Y. S., & Buyco, E. H. 1970, Thermophysical Properties of Matter Vol. 5 (New York: Plenum)

Ueta, T., Meixner, M., & Bobrowsky, M. 2000, ApJ, 528, 861

Ueta T., Meixner, M., Hinz, P. M., Hoffmann, W. F., Brandner, W., Dayal, A., Deutsch, L. K., Fazio, G. G., & Hora, J. L. 2001, ApJ, 557, 831

Wachter, A., Schröder, K.-P., Winters, J. M., Arndt, T. U., & Sedlmayr, E. 2002, A&A, 384, 452

Willson, L. A. 2000, ARA&A, 38, 573

Fig. 1.— Top: A blow up of a pair-subtracted spectrogram of IRAS 22272+5435 near 3.4 μm region. The spectrograms are recorded at two different locations of the array (position A and position B) by nodding the AO tip-tilt mirror by 2″. The two spectrogram are subtracted from each other to remove the continuum and the line emissions of the sky. Bottom: A cross-cut of the positive and negative spectrograms at 3.4 μm. The slit was put along the position angle 56° the elongation of the mid-infrared image. The apertures of 4-pixel (0.″23) in width are defined at every 2 pixel. The size and location of apertures are shown by boxes.

Fig. 2.— The spectra of IRAS 22272+5435 extracted from the apertures shown in Figure 1. Left: From the spectrogram obtained at the position A. Right: From position B. Power law continua are defined by fitting the wavelength regions free of spectral features. All spectra are normalized at 3.5 μm. The off-center spectra are offset relative to the central star spectrum for clarity, and placed at every 0.5 grid in the relative intensity unit.

Fig. 3.— Same as Figure 2, but binned by 4 pixels and the power law continua are subtracted. While the spectra close to the central star are free from dust emission features, the molecular absorption features of C_2H_2 and HCN are found (Figure 4). The broad emission features centered at 3.3 μm and 3.4 μm are of aromatic and aliphatic hydrocarbons, respectively. The off-center spectra are offset relative to the central star spectrum and placed in every 0.25 grid in the relative intensity unit.

Fig. 4.— A comparison of the 3.0 μm absorption feature of IRAS 22272+5435 at the central star with the acetylene (C_2H_2) and hydrogen cyanide (HCN) bands found in CRL 618 (Chiar et al. 1998). The C_2H_2 and HCN spectra are also calculated using the HITRAN database (Rothman et al. 1998) and shown in the bottom of the panel.

Fig. 5.— Left: A blow-up of the hydrocarbon emission features at the northeast region of the nebula. The spectra are continuum subtracted, and normalized at 3.3 μm. Right: A sequence of absorption spectra of laboratory analogs of hydrocarbon dust subject to thermal annealing (Goto et al. 2000).

Fig. 6.— A comparison of the 3.4 μm *absorption* features toward CRL 618 (Chiar et al. 1998), Galactic center source GCS 3 (Chiar et al. 2000) with the 3.4 μm *emission* feature of IRAS 22272+5435. Two types of laboratory analog from Mennella et al. (1999) and Goto et al. (2000) are shown for comparison. The dotted lines indicate the asymmetric vibrational modes of C-H bonds in methyl (3.38 μm) and methylene groups (3.42 μm), and the symmetric vibrational mode of methylene groups (3.48 μm) (Dischler, Bubenzer, & Koidl 1983).

Fig. 7.— A schematic of how the aliphatic material could be formed and preserved in the

warm circumstellar environment. A small grain starts nucleated only at far away from the star where the ambient temperature is cool enough not to destroy the aliphatic C-H bonds. The most of the grains are originated warm and close to the central star, and rapidly grows as it is blown away with mass loss wind. Because the grain growth continues until the source gas is completely depleted, the aliphatic mantles are gradually formed around their graphitized cores.

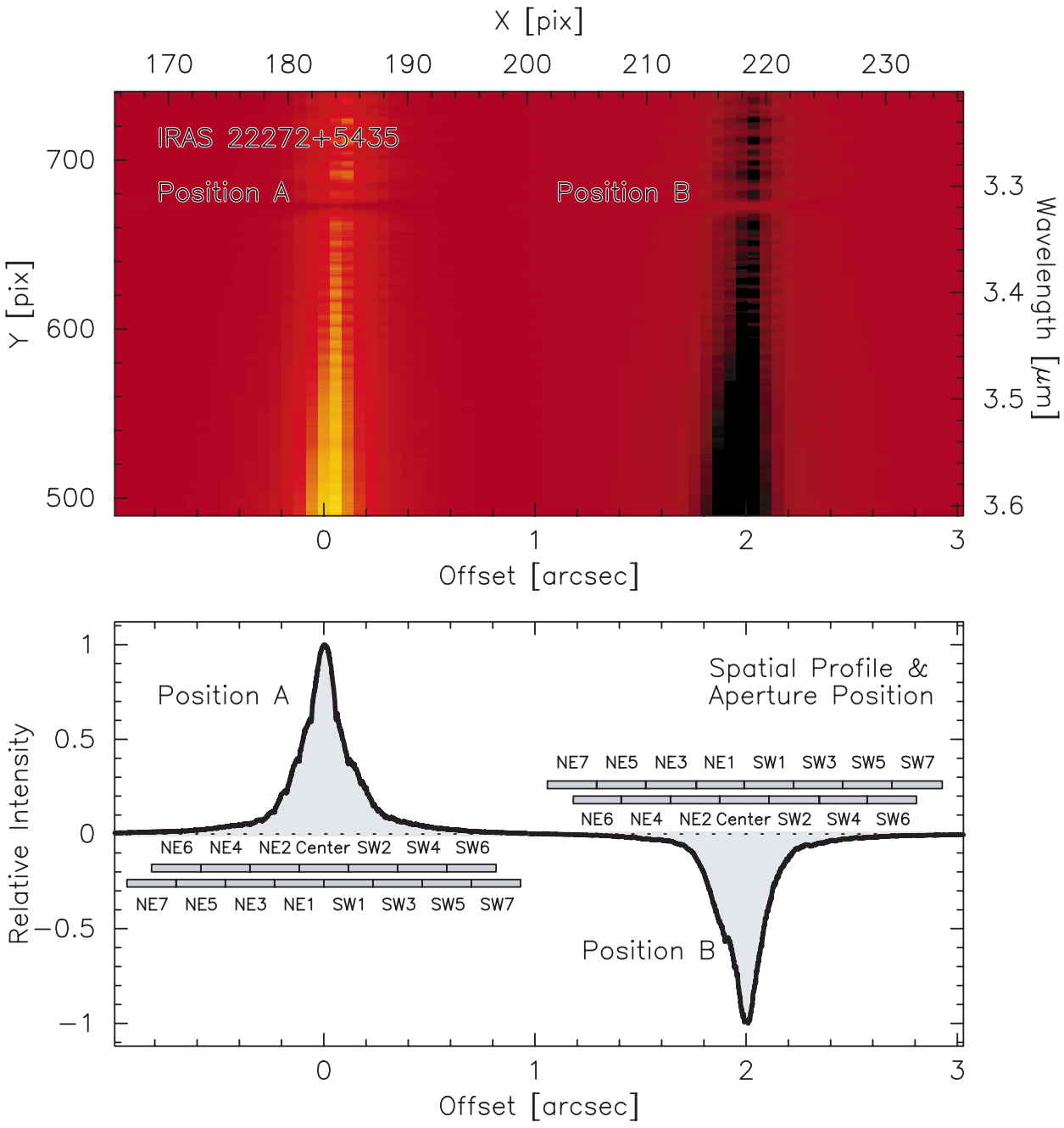

Fig. 1.—

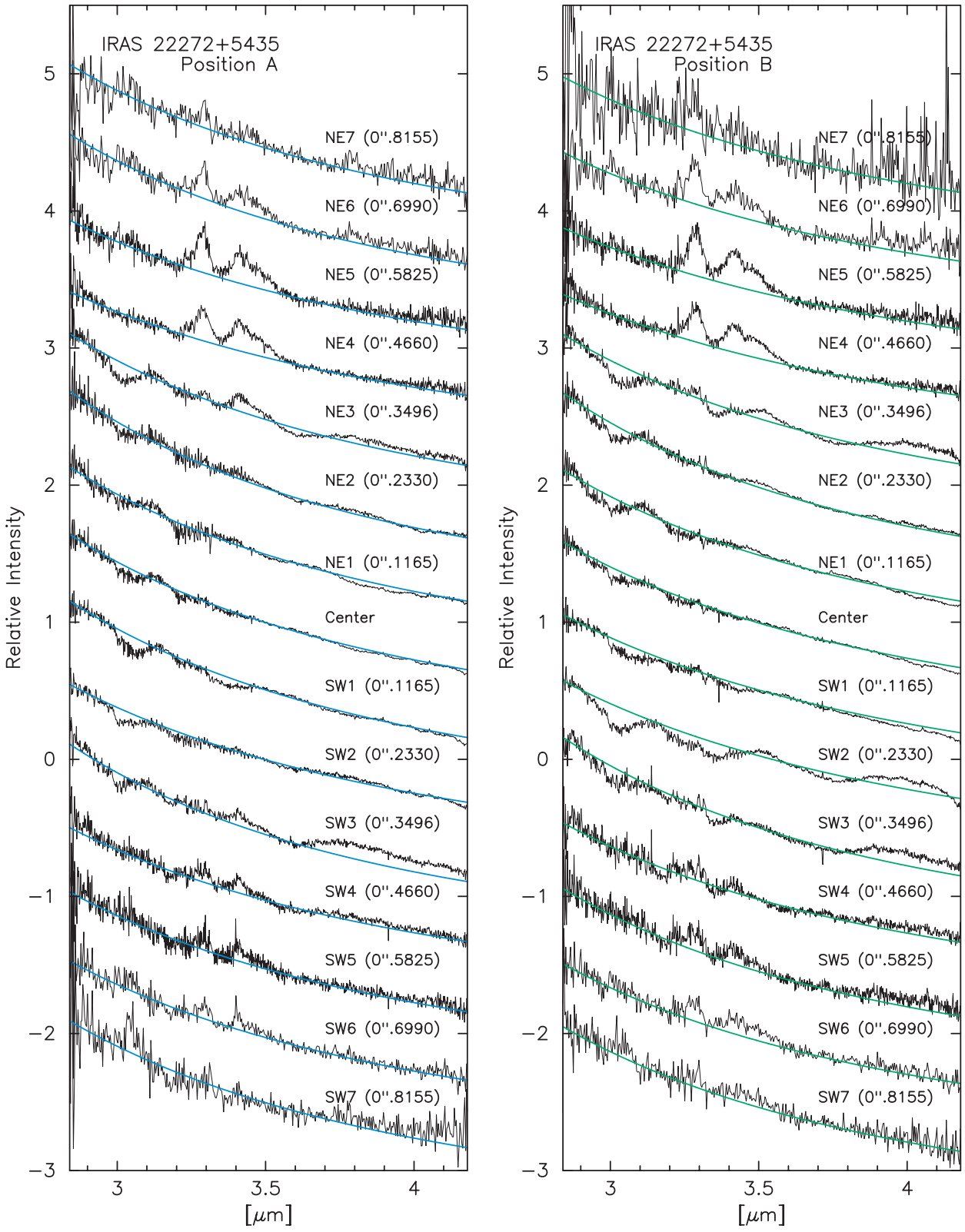

Fig. 2.—

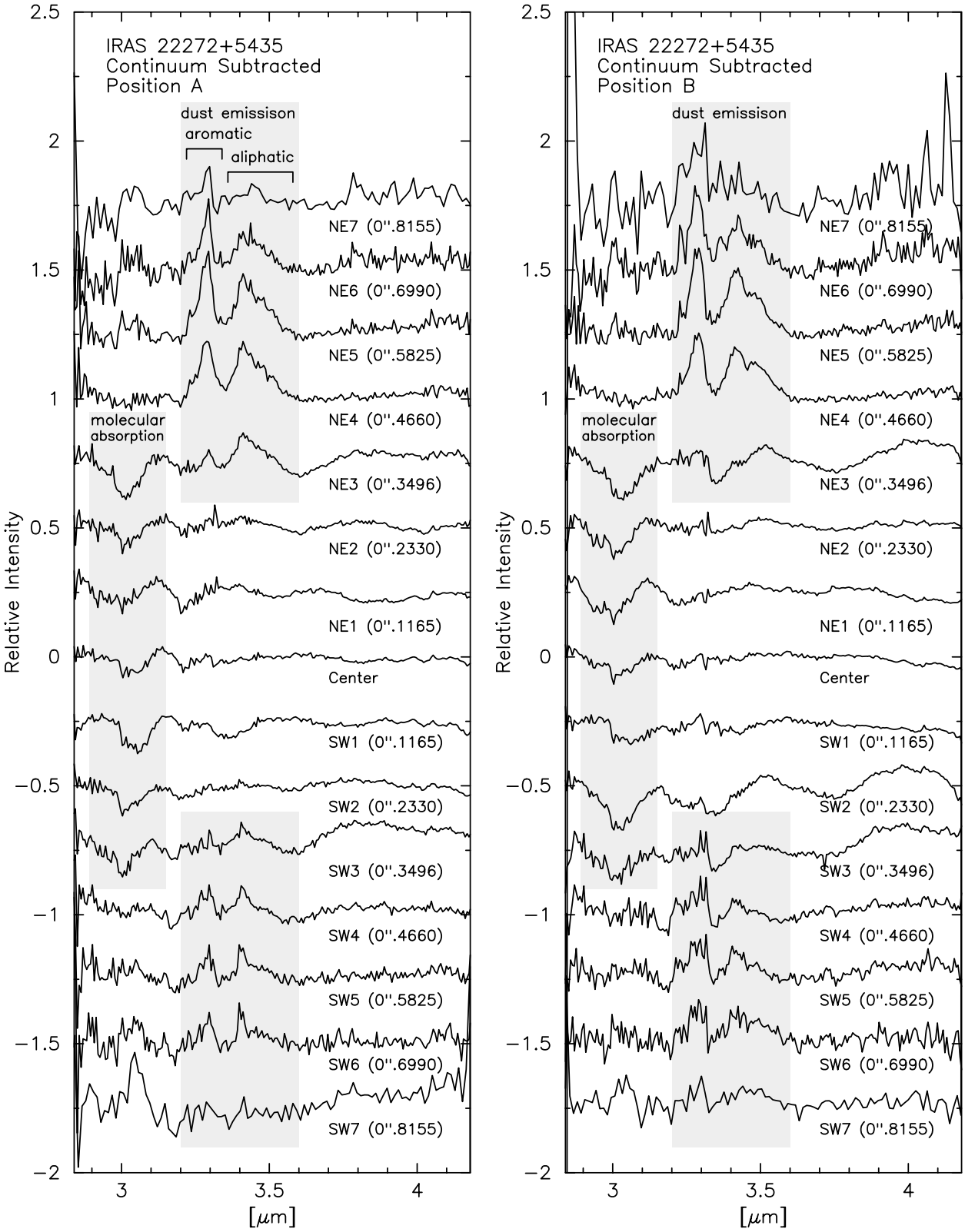

Fig. 3.—

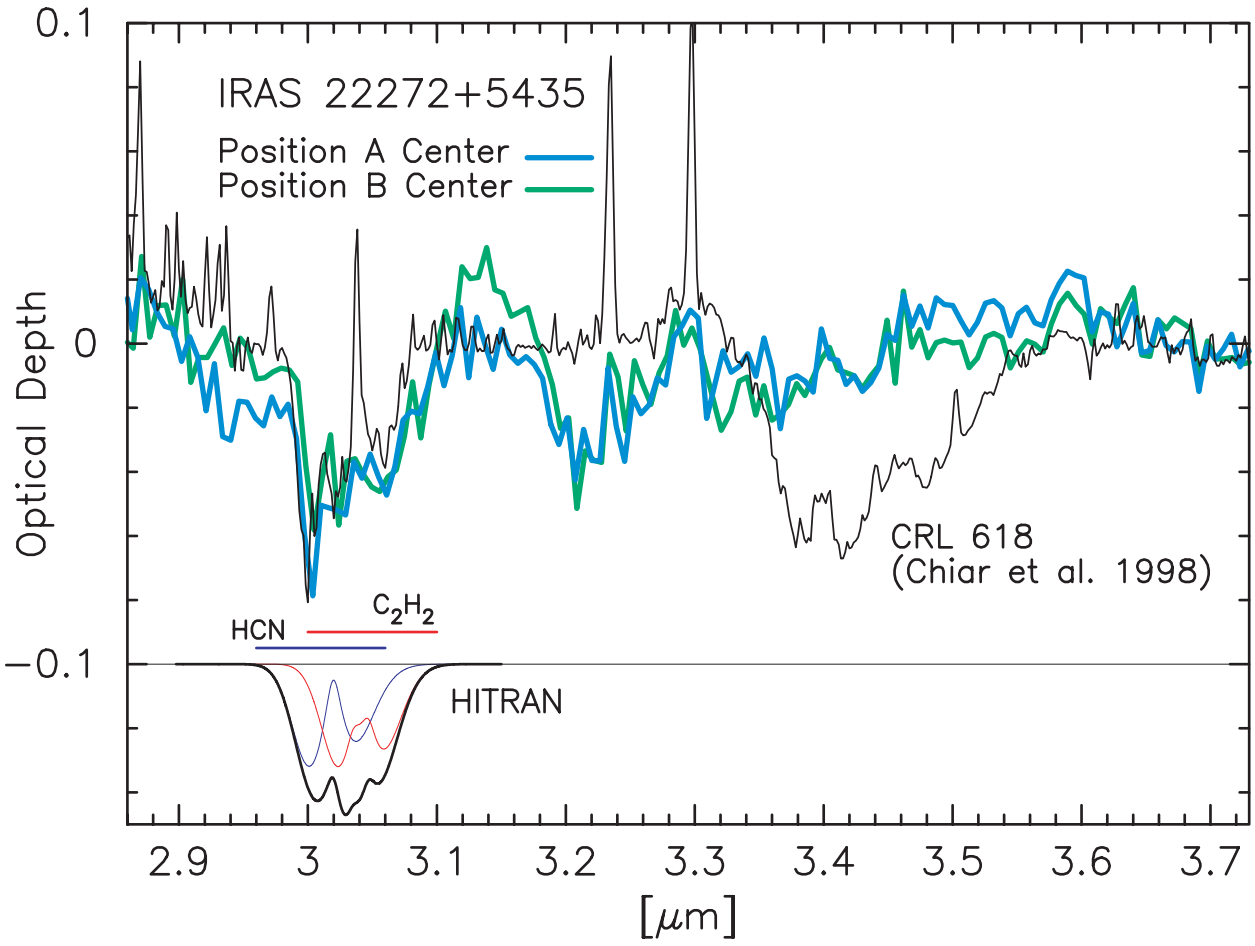

Fig. 4.—

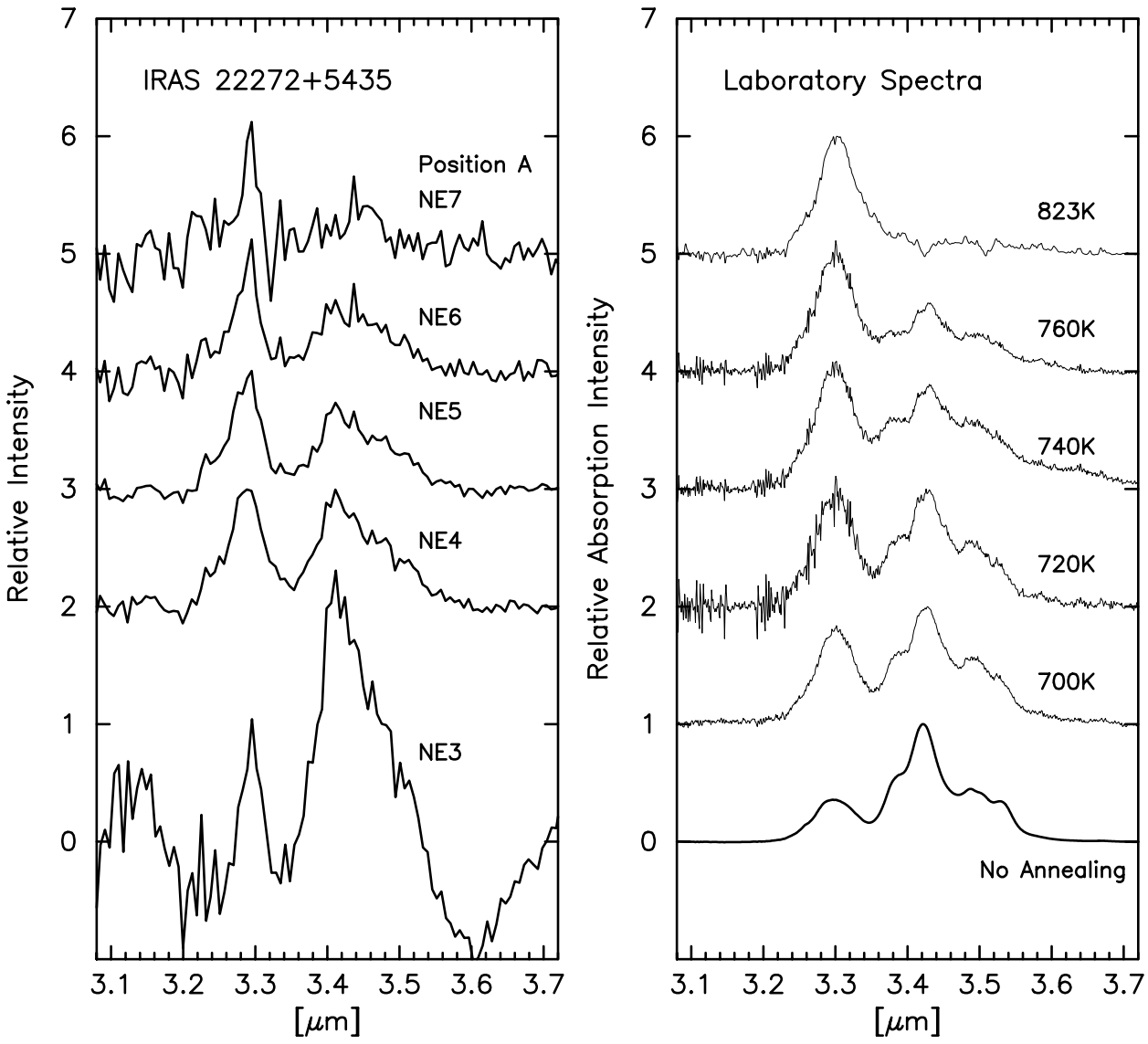

Fig. 5.—

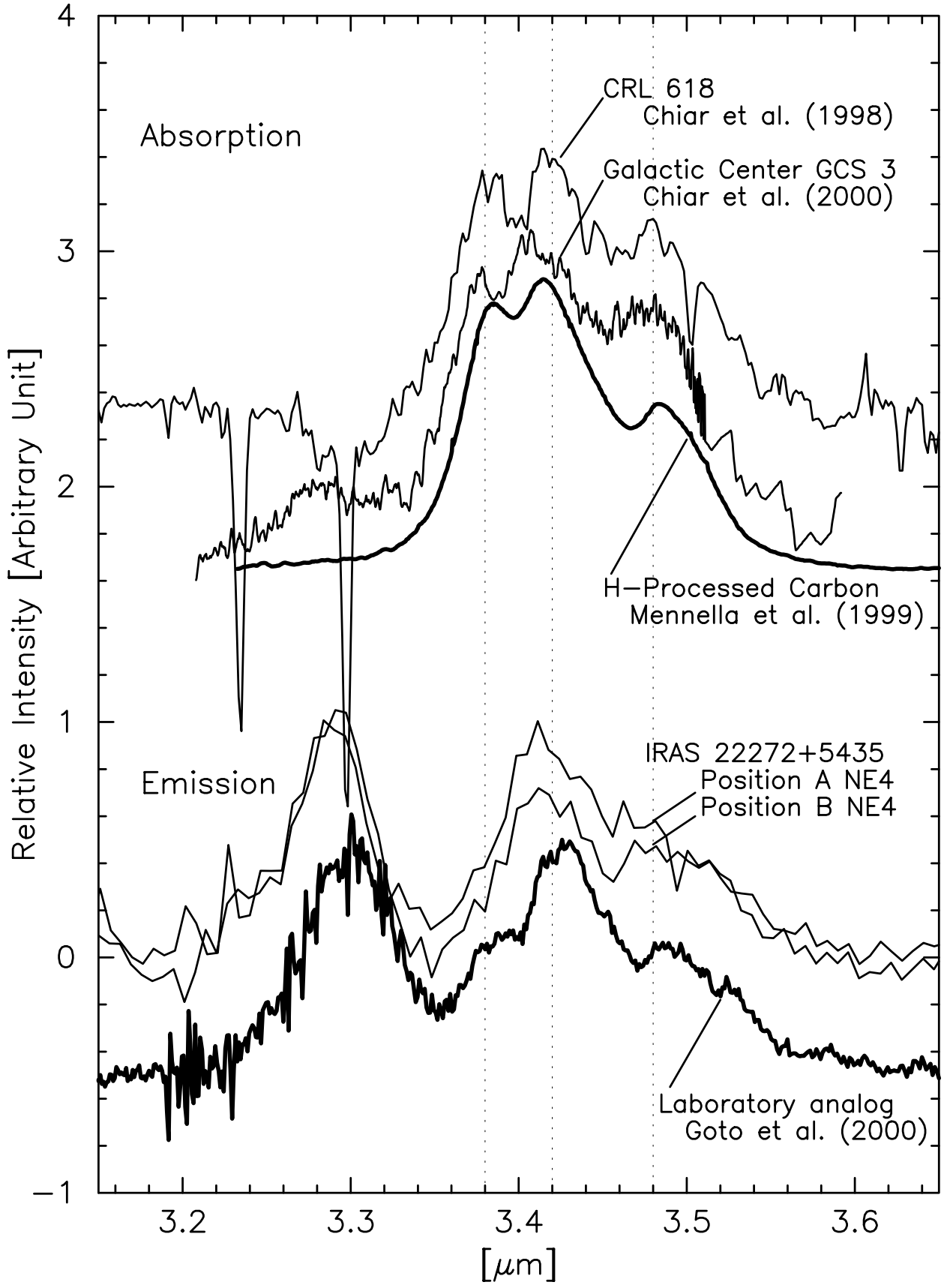

Fig. 6.—

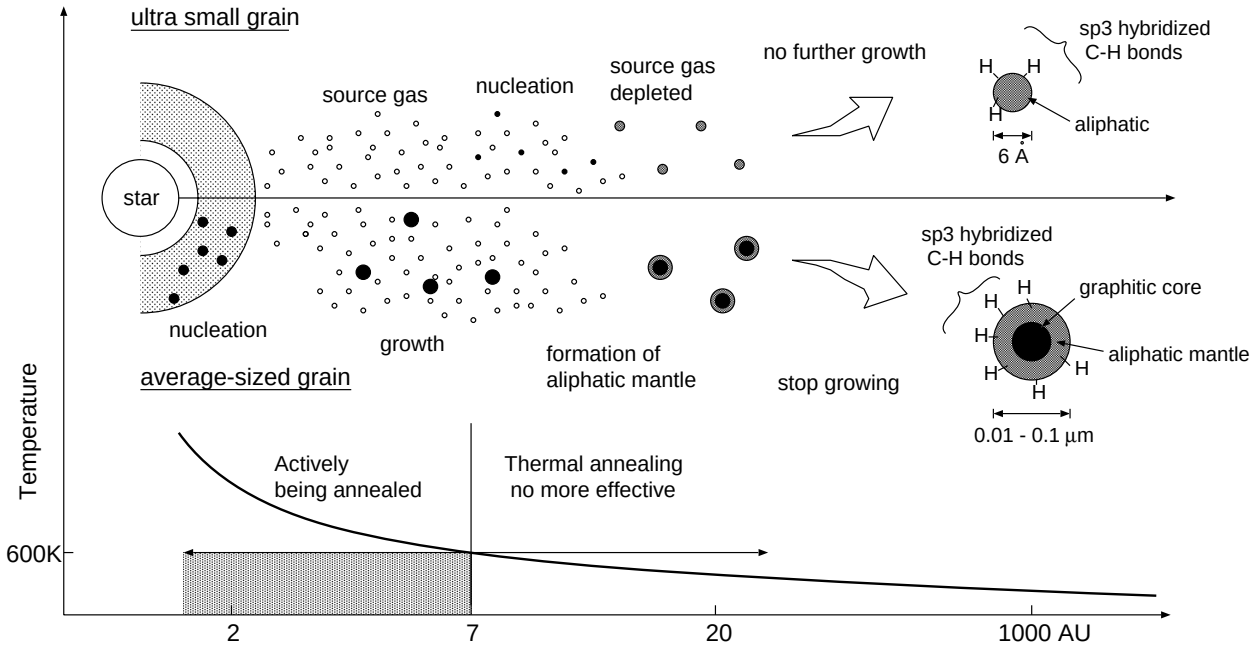

Fig. 7.—